Inorg. Chem. **2002**, *41*, 2678–2689

Photolytic Reactions of Subvalent Aluminum(I) Halides in the Presence of Dioxygen: Generation and Characterization of the Peroxo Species $XAlO_2$ and $XAl(\mu\text{-}O)_2AlX$ (X = F, Cl, Br) †

Jan Bahlo, Hans-Jörg Himmel, and Hansgeorg Schnöckel*

Lehrstuhl für Analytische Chemie, Institut für Anorganische Chemie, Universität Karlsruhe, Engesserstrasse, Geb. 30-45, 76128 Karlsruhe, Germany

Received December 27, 2001

The photolytic reactions of AlX (X = F, Cl, and Br) with O_2 in solid argon matrixes are shown to yield the peroxo species $XAlO_2$, all exhibiting C_{2v} symmetry. The species were identified and characterized by means of IR spectroscopy allied with quantum mechanical calculations. In addition to singlet $XAlO_2$ as the main product of the reaction of AlX, the experiments give clear evidence for the formation of $XAl(\mu\text{-}O)_2AlX$, by the reaction of the dimer $(AlX)_2$, which is also known to be present in the matrixes upon deposition. Finally, weak IR absorptions were tentatively assigned to $XAlO_2$ in its *triplet* electronic state. According to our calculations, the singlet–triplet gap amounts to about 40 kJ mol^{-1} for all species. The properties of the peroxide species invite comparison with previously investigated dioxygen complexes, as well as the superoxide species XAlOO and various possible products of the reaction of $(AlX)_2$ dimers.

Introduction

The incentive for studying peroxo complexes comes particularly from the role these complexes play in organic and inorganic syntheses and in biological processes, e.g., as oxygen carrier systems in oxyhemocyanin. Hemocyanin contains a dinuclear copper site capable of binding O_2 in a $\mu\text{-}\eta^2\text{:}\eta^2$ peroxo complex.[1] Among the well-known representatives of compounds that have found use as oxygen-transfer systems in preparative chemistry are the dioxiranes, $RR'CO_2$.[2] Finally, peroxo complexes are potential intermediates or products during oxidation of metals or metal clusters.[3]

Matrix isolation is now well established as a promising method for generating and characterizing peroxo and other complexes of dioxygen with small model compounds. With relevance to the present investigation, the thermal and photolytic matrix reactions of silylenes, SiX_2 (X = CH_3,[4] F, Cl[5]), Si,[6] and the groups 1,[7] 2,[8−11] and 13 elements[12−15] with O_2 have been extensively studied in the past. Here we report on the photolytically stimulated reaction of AlX (X = F, Cl, and Br) with O_2, leading to the peroxo species $XAlO_2$. Additionally, $XAl(\mu\text{-}O)_2AlX$ is shown to be formed as the only significant product of the reaction of $(AlX)_2$ with O_2. In a previous paper, IR signals were already tentatively assigned to this second product.[16] However, in light of the investigations presented here, the IR signals have to be reassigned.

† This paper is dedicated to Professor Gottfried Huttner of the University of Heidelberg to mark his 65th birthday.

* To whom correspondence should be addressed. E-mail: hansgeorg.schnoeckel@chemie.uni-karlsruhe.de.

(1) Kitajima, N.; Moro-oka, Y. *Chem. Rev.* **1994**, *94*, 737.
(2) See, for example: Adam, W.; Chan, Y.-Y.; Cremer, D.; Gauss, J.; Scheutzow, D.; Schindler, M. *J. Org. Chem.* **1988**, *53*, 3007. Baumstark, A. L.; Vasquez, P. C. *J. Org. Chem.* **1988**, *53*, 3437.
(3) Salanov, A. N.; BiBin, V. N. *Surf. Sci.* **1999**, *441*, 399.
(4) Patyk, A.; Sander, W.; Gauss, J.; Cremer, D. *Angew. Chem.* **1989**, *101*, 920.
(5) Patyk, A.; Sander, W.; Gauss, J. Cremer, D. *Chem. Ber.* **1990**, *123*, 89.
(6) Tremblay, B.; Roy, P.; Manceron, L.; Alikhani, M. E.; Roy, D. *J. Chem. Phys.* **1996**, *104*, 2773.
(7) (a) Jones, R. D.; Summerville, D. A.; Basolo, F. *Chem. Rev.* **1979**, *79*, 9, 139. (b) Giguère, P. A.; Srinivasan, T. K. K. *J. Raman Spectrosc.* **1974**, *2*, 125. (c) Nakamoto, K. *Infrared and Raman Spectra of Inorganic and Coordination Compounds Part A*, 5th ed.; Wiley-Interscience: New York, 1997; p 158 ff.
(8) Andrews, L. Chertihin, G. V.; Thompson, C. A.; Dillon, J.; Byrne, S.; Bauschlicher, C. W., Jr. *J. Phys. Chem.* **1996**, *100*, 10088.
(9) Andrews, L.; Yustein, J. T. *J. Phys. Chem.* **1993**, *97*, 12700.
(10) Andrews, L.; Yustein, J. T.; Thompson, C. A.; Hunt, R. D. *J. Phys. Chem.* **1994**, *98*, 6514.
(11) Chertihin, G. V.; Andrews, L. *J. Chem. Phys.* **1997**, *106*, 3457.
(12) Andrews, L.; Burkholder, T. R.; Yustein, J. T. *J. Phys. Chem.* **1992**, *96*, 10182.
(13) Kelsall, B. J.; Carlson, K. D. *J. Phys. Chem.* **1980**, *84*, 951−959.
(14) Burkholder, T. R.; Yustein, J. T.; Andrews, L. *J. Phys. Chem.* **1992**, *96*, 10189.
(15) Zehe, M. J.; Lynch, D. A., Jr.; Kelsall, B. J.; Carlson, K. D. *J. Phys. Chem.* **1979**, *83*, 656.
(16) (a) Ahlrichs, R.; Zhengyan, L.; Schnöckel, H. *Z. Anorg. Allg. Chem.* **1984**, *519*, 155−164.

10.1021/ic011313d CCC: $22.00
Published on Web 04/26/2002

Subvalent halides of group 13 metals such as AlX have proved to be promising educts for the synthesis of new compounds of group 13 elements.[17] For example, metastable solutions of AlX in toluene/ether give access to Al_n cluster compounds, when warmed in the presence of a suitable ligand [e.g., $N(SiMe_3)_2^-$].[18] The matrix environment offers the possibility to study the reactivity of AlX and its homologues GaX and InX in detail. One example is the photolytically induced generation of $HAlCl_2$ as the product of the matrix reaction of AlCl with HCl.[19] Photolysis will be shown also to be essential to initiate the reaction of AlX with O_2, yielding the peroxo species $XAlO_2$. The experimental results will be compared with the results of quantum mechanical calculations, and the geometries of the $XAlO_2$ species will be compared with those of other, already known peroxo species.

Experimental Section

In a vacuum apparatus, AlX (X = F, Cl, and Br) was produced by passing CHF_3 (Messer, 99.995%), HCl (Messer, 99.98%), or HBr (Messer, 99.98%) over Al (Merck, 99.999%) in a Knudsen-type graphite cell, heated resistively to 900 °C. Hence, the AlX vapor was co-deposited with an excess of O_2-doped argon on a copper block kept at 13 K by means of a closed-cycle refrigerator (Leybold LB 510). Further details of the apparatus and the matrix technique are given elsewhere.[20]

The following chemicals were used as supplied and with the quoted purities: $^{16}O_2$ (Messer, 99.9998%), $^{18}O_2$ (Prochem, 99.1%), Ar (Messer, 99.9998%).

UV photolysis (λ_{max} = 254 nm) was achieved with the aid of a low-pressure Hg lamp (Graentzel, Karlsruhe) operating at 200 W.

IR measurements were made with the use of a Bruker 113v spectrometer, equipped with an MCT detector and a DTGS detector. The spectra were taken with a resolution of 0.5 cm^{-1} for measurements with the MCT detector and 1.0 cm^{-1} for measurements with the DTGS detector.

The quantum chemical calculations were generally performed with the use of density functional theory (DFT) calculations relying on the GAUSSIAN98 program package,[21] and the B3LYP method in combination with a 6-311G(d) basis set was used. Additional ab initio (MP2) calculations were carried out with the aid of the RIMP2 module[22] of the TURBOMOLE program package[23] and a TZVPP-type basis set.

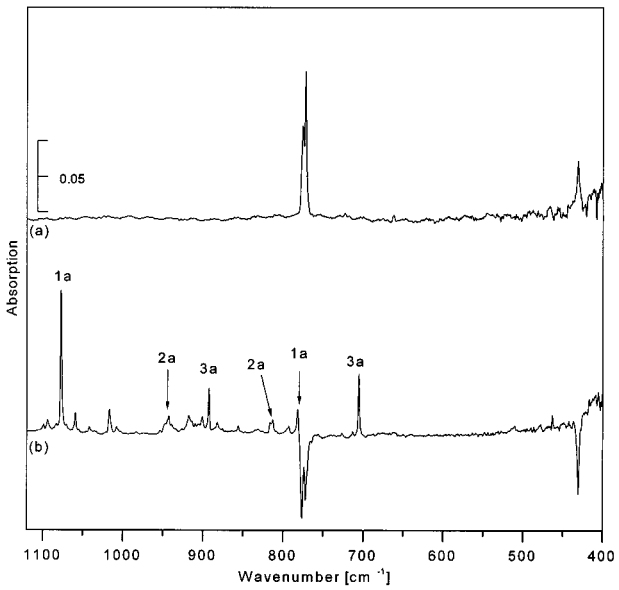

Figure 1. IR spectra for the reaction of AlF with $^{16}O_2$: (a) spectrum taken upon co-condensation of AlF with 5% $^{16}O_2$ in Ar, (b) spectrum following photolysis of the matrix with λ = 254 nm light.

Results

The photolytically induced reaction of AlX (X = F, Cl, and Br) with O_2 was followed using IR spectroscopy, and the products were identified on the basis of (i) experiments in which the O_2 concentration was varried (1−15% in Ar), (ii) experiments with different isotopomers ($^{16}O_2$, $^{18}O_2$, and $^{16}O_2/^{18}O_2$ and $^{16}O_2/^{16}O^{18}O/^{18}O_2$ mixtures), and (iii) the selection rules expected to govern the signal intensities.

AlF + O_2. The IR spectra of an Ar matrix containing AlF and 5% $^{16}O_2$ are shown in Figure 1. The spectrum obtained after co-deposition of AlF and O_2 gives clear evidence of two signals located at 772/778 and 431 cm^{-1} which were previously identified with AlF and its dimer $(AlF)_2$, respectively.[16] Besides these two strong signals, the spectrum contains weak signals due to traces of CHF_3[24] and impurities (H_2O, CO, CO_2)[25] which can be reduced to a minimum but never completely excluded.

Following 20 min of photolysis at λ_{max} = 254 nm, the spectrum witnessed the decrease of the signals due to AlF and $(AlF)_2$. At the same time, several new signals were observed to develop. A first group of signals, belonging to a common absorber, **1a**, consists of two strong signals at 1077.3 and 781.8 cm^{-1}. A second group of signals, observed at 942.8 and 812.9 cm^{-1}, belongs to a second product, **2a**. Moreover, the spectrum witnessed the appearance of signals at 892.4 and 705.3 cm^{-1} due to a third distinct species, **3a**.

(17) Dohmeier, C.; Loos, D.; Schnöckel, H. *Angew. Chem., Int. Ed. Engl.* **1996**, *35*, 129.
(18) Klemp, C.; Köppe, R.; Weckert, E.; Schnöckel, H. *Angew. Chem.* **1999**, *111*, 1851; *Angew. Chem., Int. Ed.* **1999**, *38*, 1739. Ecker, A.; Weckert, E.; Schnöckel, H. *Nature* **1997**, *387*, 379. Köhnlein, H.; Stösser, G.; Baum, E.; Möllhausen, E.; Huniar, U.; Schnöckel, H. *Angew. Chem.* **2000**, *112*, 828; *Angew. Chem., Int. Ed.* **2000**, *39*, 799. Köhnlein, H.; Purath, A.; Klemp, C.; Baum, E.; Krossing, I.; Stösser, G.; Schnöckel, H. *Inorg. Chem.* **2001**, *40*, 4830−4838.
(19) Schnöckel, H *J. Mol. Struct.* **1978**, *50*, 275.
(20) Schnöckel, H. *J. Mol. Struct.* **1978**, *50*, 267.
(21) GAUSSIAN 98, Revision A.3: Frisch, M. J.; Trucks, G. W.; Schlegel, H. B.; Scuseria, G. E.; Robb, M. A.; Cheeseman, J. R.; Zakrzewski, V. G.; Montgomery, J. A., Jr.; Stratmann, R. E.; Burant, J. C.; Dapprich, S.; Millam, J. M.; Daniels, A. D.; Kudin, K. N.; Strain, M. C.; Farkas, O.; Tomasi, J.; Barone, V.; Cossi, M.; Cammi, R.; Mennucci, B.; Pomelli, C.; Adamo, C.; Clifford, S.; Ochterski, J.; Petersson, G. A.; Ayala, P. Y.; Cui, Q.; Morokuma, K.; Malick, D. K.; Rabuck, A. D.; Raghavachari, K.; Foresman, J. B.; Cioslowski, J.; Ortiz, J. V.; Stefanov, B. B.; Liu, G.; Liashenko, A.; Piskorz, P.; Komaromi, I.; Gomperts, R.; Martin, R. L.; Fox, D. J.; Keith, T.; Al-Laham, M. A.; Peng, C. Y.; Nanayakkara, A.; Gonzalez, C.; Challacombe, M.; Gill, P. M. W.; Johnson, B.; Chen, W.; Wong, M. W.; Andres, J. L.; Gonzalez, C.; Head-Gordon, M.; Replogle, E. S.; Pople, J. A. Gaussian Inc.: Pittsburgh, PA, 1998.
(22) Eichhorn, K.; Treutler, O.; Öhm, H.; Häser, M.; Ahlrichs, R. *Chem. Phys. Lett.* **1995**, *240*, 283.
(23) Treutler, O.; Ahlrichs, R. *J. Chem. Phys.* **1995**, *102*, 346.
(24) Ruof, A.; Bürger, H.; Biedermann, S. *Spectrochim. Acta* **1971**, *27A*, 1359.
(25) Ayers, G. P.; Pullin, A. D. E. *Spectrochim. Acta* **1976**, *32A*, 1629, 1689. Jiang, G. J.; Person, W. B.; Brown, K. G. *J. Chem. Phys.* **1975**, *62*, 1201. Toth, R. A. *J. Mol. Spectrosc.* **1974**, *53*, 1.

Table 1. Infrared Absorptions Associated with the Products of AlF with $^{16}O_2$, $^{18}O_2$, $^{16}O_2/^{18}O_2$, and $^{16}O_2/^{16}O^{18}O/^{18}O_2$ (in cm^{-1})

$^{16}O_2$	$^{18}O_2$	$^{16}O_2/^{18}O_2$	$^{16}O_2/^{16}O^{18}O/^{18}O_2$	absorber
1077.3		1077.3	1077.3	singlet $FAlO_2$, **1a**
			1070.7	
	1063.6	1063.6	1063.6	
1059.3	1044.8			triplet $FAlO_2$
1042.3	1026.7		1033.4	
1016.9	1003.5		1008.6	
942.8		942.8	942.8	$FAl(\mu\text{-}O)_2AlF$, **2a**
		(939.6)	939.2	
	936.2	936.0	936.0	
892.4		892.4	892.4	species with four O
			889.7	atoms, $FAlO_4$, **3a**
		887.6	887.6	
			885.9	
	883.7	883.7	883.7	
812.9		812.9	812.9	$FAl(\mu\text{-}O)_2AlF$, **2a**
			802.7	
	785.6	785.6	785.6	
781.8		781.8	781.8	singlet $FAlO_2$, **1a**
			766.8	
	747.9	747.9	747.9	
705.3		705.3	705.6	species with four O
			701.5	atoms, $FAlO_4$, **3a**
		697.9	697.9	
			693.5	
	689.9	689.8	689.8	

Finally, a weak feature appearing at 917.9 cm^{-1} must be associated with another product of the reaction with O_2.

Experiments with $^{18}O_2$ in place of $^{16}O_2$ gave again no evidence for any reaction products upon co-deposition. In the spectrum following photolysis all the signals due to species **1a**, **2a**, and **3a** were observed to be shifted to lower wavenumber (see Table 1). With wavenumbers of 1063.6 and 747.9 cm^{-1}, the signals due to species **1a** were shifted by 13.7 cm^{-1} [$\nu(^{16}O)/\nu(^{18}O) = 1.0132$] and 33.9 cm^{-1} [$\nu(^{16}O)/\nu(^{18}O) = 1.0455$], respectively. The ratios will be compared to the calculated ones in the Discussion. The signals due to species **2a** exhibited shifts of 6.6 and 27.3 cm^{-1}, corresponding to $\nu(^{16}O)/\nu(^{18}O)$ ratios of 1.0065 and 1.0348. The signals assigned to species **3a** were shifted to 883.7 cm^{-1} [$\nu(^{16}O)/\nu(^{18}O) = 1.0102$] and 689.9 cm^{-1} [$\nu(^{16}O)/\nu(^{18}O) = 1.0232$]. The weak signal at 917.9 cm^{-1} in the experiments with $^{16}O_2$ was observed at 899.7 cm^{-1} [$\nu(^{16}O)/\nu(^{18}O) = 1.0202$].

The experiments were also repeated using 1:1 mixtures of $^{16}O_2/^{18}O_2$ and 1:2:1 mixtures of $^{16}O_2/^{16}O^{18}O/^{18}O_2$. In the experiments with $^{16}O_2/^{18}O_2$, the signals due to species **1a** were the superposition of the signals observed in the experiments using $^{16}O_2$ and $^{18}O_2$ alone (see Figure 2). Thus, doublet signals at 1077.3/1063.6 and 781.8/747.9 cm^{-1} appeared upon photolysis of the matrix. **2a** was the author of two doublet features at 942.8/936.2 and 812.9/785.6 cm^{-1}. It follows that **1a** and **2a** contain *two* equivalent O atoms. By contrast, species **3a** gave rise to extra signals that could not be accounted for merely by the superposition of the signals observed in the experiments using $^{16}O_2$ and $^{18}O_2$ separately. Thus, this species is the product of the reaction of *more than one* O_2 molecule. In the experiments with $^{16}O_2/^{16}O^{18}O/^{18}O_2$ mixtures the two vibrational modes of **1a** were both split into triplets positioned at 1077/1070/1063 and 781/767/747 cm^{-1}. The bands due to **2a** also showed triplet patterns, with the signals due to the $^{16}O^{18}O$ form of species **2a** appearing at 939.4 and 802.7 cm^{-1}. The fates of all the signals are summarized in Table 1.

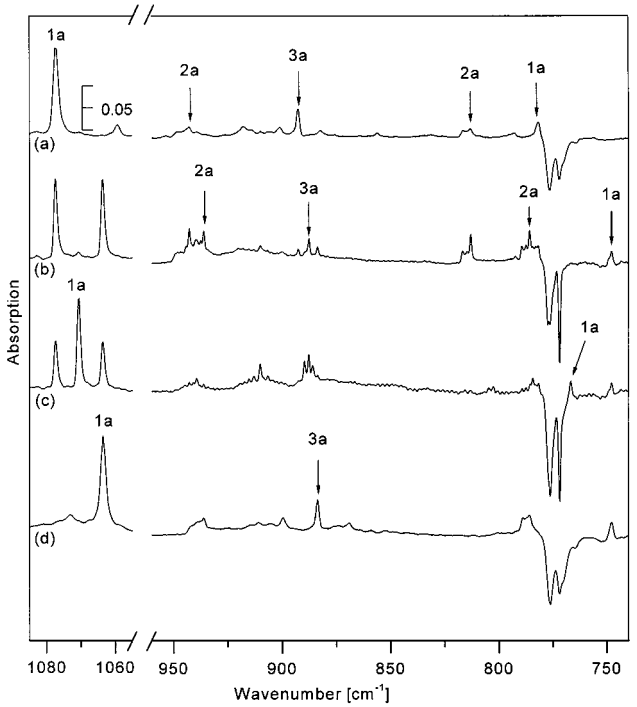

Figure 2. Spectra taken following photolysis of matrixes containing AlF and (a) 5% $^{16}O_2$, (b) mixtures of $^{16}O_2$ and $^{18}O_2$ (5% in total), (c) 1:2:1 mixtures of $^{16}O_2$, $^{16}O^{18}O$, and $^{18}O_2$ (5% in total), and (d) 5% $^{18}O_2$ in solid argon (spectra b and c scaled by a factor of 2).

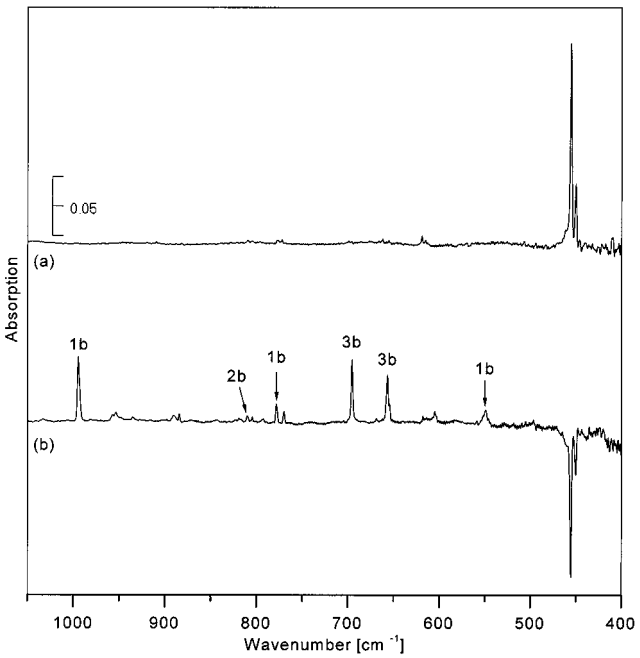

Figure 3. IR spectra for the reaction of AlCl with $^{16}O_2$: (a) spectrum taken upon co-condensation of AlCl with 5% $^{16}O_2$ in Ar, (b) spectrum following photolysis of the matrix with $\lambda = 254$ nm light.

AlCl + O_2. Figure 3 shows the spectra taken for the matrix reaction of AlCl with $^{16}O_2$. The spectrum taken upon co-deposition again leaked any sign of a reaction product. It was dominated by an intense signal at 455 cm^{-1} due to AlCl.[26] The wavenumbers of the IR-active vibrational modes

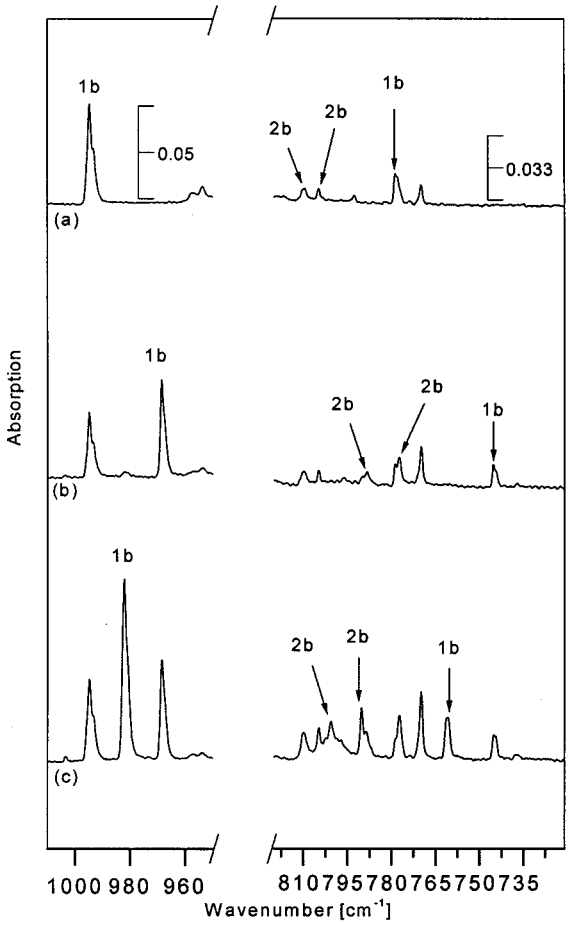

Figure 4. Spectra taken following photolysis of matrixes containing AlCl and (a) 5% $^{16}O_2$, (b) mixtures of $^{16}O_2$ and $^{18}O_2$ (5% in total), and (c) 1:2:1 mixtures of $^{16}O_2$, $^{16}O^{18}O$, and $^{18}O_2$ (5%) in Ar.

of the dimer $(AlCl)_2$[17,26] are out of the range of detection in our experiments.

Upon photolysis at $\lambda_{max} = 254$ nm, three strong absorptions were observed to grow in. With positions of 994.6, 778.7, and 549.3 cm^{-1}, the author of these absorptions is in all probability the Cl-equivalent **1b** of product **1a**. Another set of signals, located at 809.8 and 804.7 cm^{-1}, belong to a second absorber, **2b**. Additionally, a small and somewhat broader signal was observed at 957.4/953.4 cm^{-1}, and the spectrum also included signals at 695.8 and 656.6 cm^{-1} due to another species, **3b**. The last signal showed a shoulder at 654.4 cm^{-1}, which can be assigned to traces of $HAlCl_2$.[19]

The experiments with $^{18}O_2$ followed the same pattern. With wavenumbers of 968.3, 745.0, and 518.5 cm^{-1}, the three signals due to **1b** were shifted by 26.3 cm^{-1} [$\nu(^{16}O)/\nu(^{18}O) = 1.0272$], 32.2 cm^{-1} [$\nu(^{16}O)/\nu(^{18}O) = 1.0432$], and 30.8 cm^{-1} [$\nu(^{16}O)/\nu(^{18}O) = 1.0594$], respectively. The signals due to species **2b** were observed at 788.5 and 777.1 cm^{-1}, and the feature at 957.4/953.4 cm^{-1} shifted to 923.2/916.9 cm^{-1} [$\nu(^{16}O)/\nu(^{18}O) = 1.0370/1.0398$].

In the experiments using a 1:1 mixture of $^{16}O_2$ and $^{18}O_2$, doublets at 994.6/968.3, 777.2/745.0, and 549.3/518.5 cm^{-1} characterize **1b** in either its ^{16}O or its ^{18}O version (see Figure 4), whereas similar features at 809.8 and 788.5 cm^{-1} characterize **2b**. In the experiments using 1:2:1 mixtures of $^{16}O_2/^{16}O^{18}O/^{18}O_2$, additional signals were observed for all the species. The wavenumbers are given in Table 2. For example, species **2b** in its $^{16}O^{18}O$ form displays two absorptions at 800.3 and 790.3 cm^{-1}.

Table 2. Infrared Absorptions Associated with the Products of AlCl with $^{16}O_2$, $^{18}O_2$, $^{16}O_2/^{18}O_2$, and $^{16}O_2/^{16}O^{18}O/^{18}O_2$ (in cm^{-1})

$^{16}O_2$	$^{18}O_2$	$^{16}O_2/^{18}O_2$	$^{16}O_2/^{16}O^{18}O/^{18}O_2$	absorber
1964.9				$HAlCl_2$
1928.1				H_2AlCl
1916.1				
994.6		994.6	994.6	singlet $ClAlO_2$, **1b**
			982.1	
	968.3	968.3	968.3	
957.4	923.2	957.4	957.4	triplet $ClAlO_2$
953.4	916.9	953.4	953.4	
		939.2	939.2	
		942.7	942.7	
809.8		809.8	809.8	$ClAl(\mu\text{-}O)_2AlCl$, **2b**
			800.3	
	788.5	788.5	788.5	
804.7		804.7	804.7	$ClAl(\mu\text{-}O)_2AlCl$, **2b**
			790.3	
	777.1	777.1	777.1	
778.7		778.7	778.2	singlet $ClAlO_2$, **1b**
			761.0	
	745.0	745.0	745.0	
769.7				H_2AlCl
695.8		695.8	695.8	species with four O
			692.2	atoms, $ClAlO_4$, **3b**
		688.8	688.3	
			684.6	
	680.5	680.5	680.5	
656.6		656.6	656.6	species with four O
654.6	654.6	654.6	653.6	atoms, $ClAlO_4$, **3b**,
			652.7	and H_2AlCl
	650.4	650.4	650.5	

AlBr + O_2. The course of action was found to be similar to that with AlF or AlCl. Prior to photolysis, a strong signal at 357.6 cm^{-1} gave evidence for the presence of isolated AlBr molecules in the matrix. The spectrum taken after photolysis at $\lambda_{max} = 254$ nm for a matrix containing AlBr[26] and $^{16}O_2$ was dominated by signals at 972.4, 774.0, and 524.2 cm^{-1} due to a distinct product, **1c** (see Figure 5). Two absorptions belonging to **2c** were located at 800.9 and 790.2 cm^{-1}. Product **3c**, showing the hallmarks of a species containing more than two O atoms on the basis of the experiments with different isotopomers, was the author of signals at 691.6 and 618.3 cm^{-1}. Finally, the spectrum contained a weak signal at 897.8 cm^{-1}. The results of the experiments with $^{18}O_2$, $^{16}O_2/^{18}O_2$, and $^{16}O_2/^{16}O^{18}O/^{18}O_2$ are summarized in Table 3. Thus, all the signals were observed to undergo shifts upon ^{18}O substitution. The three signals due to **1c** in its ^{18}O version exhibited shifts of −25.5, −33.0, and −23.4 cm^{-1}, corresponding to $\nu(^{16}O)/\nu(^{18}O)$ ratios of 1.0269, 1.0445, and 1.0467 for the signals at 972.4, 774.0, and 524.2 cm^{-1}, respectively. In its $^{16}O^{18}O$ version, **2c** gave rise to signals at 960.7, 756.3, and 512.1 cm^{-1}. These three signals were also observed in experiments with $^{16}O_2/^{18}O_2$ mixtures, in addition to those due to **2c** in its $^{16}O_2$ and $^{18}O_2$ versions for photolysis times of 40 min and more (see Figure 6). The signals due to species **2c** in its ^{18}O version appeared at 763.1 and 774.7 cm^{-1} [$\nu(^{16}O)/\nu(^{18}O) = 1.0355$ and 1.0712, respectively]. The weak signal at 897.8 cm^{-1} shifted to 868.7 cm^{-1} in the experiments with $^{18}O_2$ [$\nu(^{16}O)/\nu(^{18}O) = 1.03349$].

(26) Schnöckel, H. *Z. Naturforsch., B* **1976**, *31*, 1291.

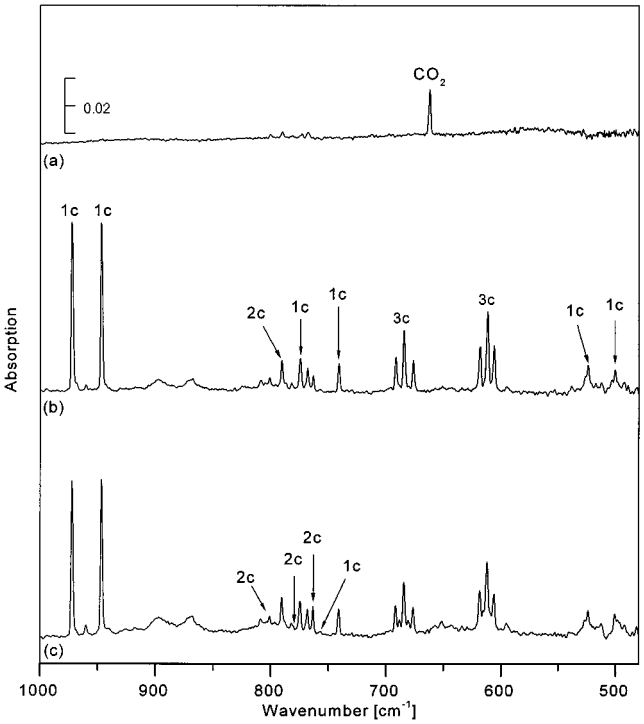

Figure 5. IR spectra for the reaction of AlBr with $^{16}O_2$: (a) spectrum taken upon co-condensation of AlBr with $^{16}O_2$ and $^{18}O_2$ (5% in total) in Ar, (b) spectrum following 10 min of photolysis of the matrix with λ = 254 nm light, (c) spectrum following another 40 min of photolysis at λ = 254 nm.

Table 3. Infrared Absorptions Associated with the Products of AlBr with $^{16}O_2$, $^{18}O_2$, $^{16}O_2/^{18}O_2$, and $^{16}O_2/^{16}O^{18}O/^{18}O_2$ (in cm^{-1})

$^{16}O_2$	$^{18}O_2$	$^{16}O_2/^{18}O_2$	$^{16}O_2/^{16}O^{18}O/^{18}O_2$	absorber
972.4		972.4	972.4	singlet, $BrAlO_2$, **1c**
			960.7	
	946.9	946.9	946.9	
897.8	868.7	897.8	897.8	triplet $BrAlO_2$
		868.7	868.7	
800.9		800.9	800.9	$BrAl(\mu\text{-}O)_2AlBr$, **2b**
	774.7	774.7	774.7	
790.2		790.2	790.2	$BrAl(\mu\text{-}O)_2AlBr$, **2b**
			780.4	
	763.1	763.1	763.1	
774.0		774.0	774.0	singlet $BrAlO_2$, **1c**
			756.3	
	741.0	741.0	741.0	
691.6		691.6	691.6	species with four O
			683.9	atoms, $BrAlO_4$, **3c**
	676.2	676.2	676.2	
618.3		618.3	618.3	species with four O
			611.3	atoms, $BrAlO_4$, **3c**
	605.7	605.7	605.7	
524.2		524.2	524.2	singlet $BrAlO_2$, **1c**
			512.5	
	500.8	500.8	500.8	

Discussion

It will be shown, on the basis of the experimental results allied (i) with the results of quantum mechanical calculations and (ii) with analogies with other known peroxo species, that the products **1a**−**1c** are the peroxo species $XAlO_2$ (X = F, Cl, and Br, structure **A**) in their singlet electronic ground states, all exhibiting C_{2v} symmetry. Species **2a**−**2c** can be identified as the products of the reaction of $(AlX)_2$ with O_2, namely, $XAl(\mu\text{-}O)_2AlX$ (structure **E**). The weak signals at 1042.3, 957.4/953.4, and 897.8 cm^{-1} in the experiments with

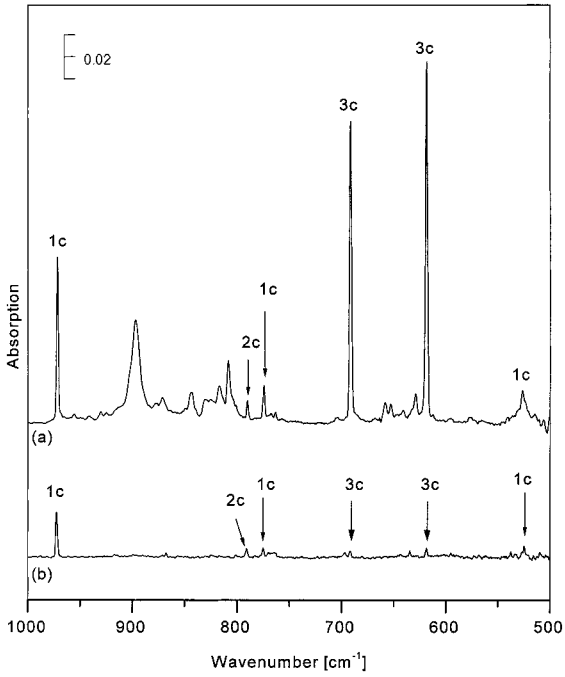

Figure 6. IR spectra for concentrations of (a) 1% and (b) 15% $^{16}O_2$ and for the reaction with AlBr following UV photolysis.

X = F, Cl, and Br, respectively, may be tentatively assigned to the peroxo species $XAlO_2$ in their triplet electronic states, formed, however, in much lower yields than **1a**−**1c**. All these species are the products of the reaction of AlX with one O_2 molecule. Species **3a**−**3c** are the products of the reaction with more than one O_2 molecule and will be discussed in detail elsewhere.[27] Here we concentrate on the reactions with only *one* O_2 molecule.

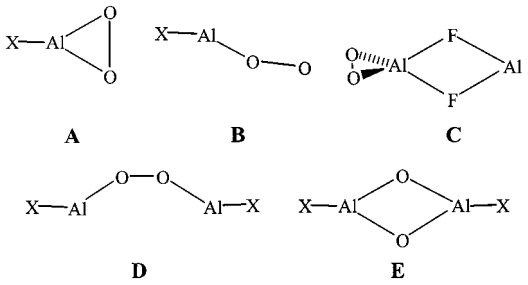

The spectra taken upon co-deposition show that not only the monomer AlF but also the dimer $(AlF)_2$ is present in the matrix, and that both are engaged in reactions with O_2 following photolysis. The same behavior is likely to occur for AlCl and AlBr, where the IR-active absorptions of the dimers are below the lower threshold of detection in our experiments (200 cm^{-1}). Our DFT calculations give the following wavenumbers (cm^{-1}) [intensities (km mol^{-1}) and symmetry assignment in parentheses] for AlF and $(AlF)_2$: 788.6 (95) for AlF and 501.8 (0, a_g), 444.8 (455, b_{1u}), 409.3 (45, b_{2u}), 347.5 (0, a_g), 253.3 (0, b_{3g}), and 138.7 (0.1, b_{3u}) for $(AlF)_2$ (in previous notations, the b_{1u}, b_{2u}, b_{3u}, and b_{3g} modes were quoted as b_{2u}, b_{3u}, b_{1u}, and b_{1g}, respectively[28]).

(27) Bahlo, J.; Himmel, H.-J.; Schnöckel, H. *Inorganic Chemistry*, submitted for publication.

Thus, the intensity of the b_{1u} absorption of $(AlF)_2$ is higher by a factor of 4.8 than that anticipated for the unique fundamental of AlF. An indication of the molecular ratio n[AlF]/n[$(AlF)_2$] can be obtained by comparison of the calculated and observed relative intensities of the absorptions. On the basis of this comparison, the matrixes contained 14 times more AlF than $(AlF)_2$. We anticipate the ratios n[AlX]/n[$(AlX)_2$] to be even larger for X = Cl and Br. Therefore, the reactions of the dimer can play but a minor role in the overall course of events. Nevertheless, the following discussion includes not only species containing *one* Al and X atom (structures **A** and **B**), but also species with *two* Al and X atoms (structures **C**−**E**). Furthermore, we will show that both triplet and singlet electronic states need to be considered. We will now discuss the experimental and theoretical results for all these species in turn.

Singlet $XAlO_2$, 1a−1c. As already mentioned, the IR signals at 1077.3 and 781.8 cm^{-1} in the experiments with AlF, at 994.6, 778.7, and 549.3 cm^{-1} in the experiments with AlCl, and at 972.4, 774.0, and 524.2 cm^{-1} in the experiments with AlBr can be assigned to the common absorbers **1a**−**1c**, respectively. The experiments with $^{16}O_2/^{18}O_2$ mixtures and with $^{16}O^{18}O$ show that each of these species contains two equivalent O atoms. The absence of any signal due to the $^{16}O/^{18}O$ versions of **1a**−**1c** in experiments with $^{16}O_2/^{18}O_2$ indicates that, as expected, the reaction is concerted. That **1a**−**1c** are the products of a reaction of only *one* O_2 molecule is also in agreement with the experiments carried out for different O_2 concentrations, where it was apparent that the products **1a**−**1c** were dominant at low O_2 concentrations (1%) while the products **3a**−**3c** were favored at high O_2 concentrations (5%). These experimental results reduce the possible candidates for **1a**−**1c** to the peroxo species $XAlO_2$ (structure **A**) or the products $Al(\mu\text{-}X)_2AlO_2$ (structure **C**), XAlOOAlX (structure **D**), and $XAl(\mu\text{-}O)_2AlX$ (structure **E**) with two bridging O atoms, depending on whether **1a**−**1c** are the products of the reaction of AlX or of its dimer $(AlX)_2$. In a previous paper,[16] the signal at 1077.3 cm^{-1} was assigned somewhat tentatively to the reaction product of the dimer $(AlF)_2$ with O_2, $FAl(\mu\text{-}O)_2AlF$. At this point the comparison of the observed IR wavenumbers with those predicted by quantum chemical calculations is of importance to reach a final decision. As shown below, on the basis of this comparison, **1a**−**1c** can be clearly identified as the peroxo species $XAlO_2$ each in its singlet electronic ground state. In a preliminary work, we have already assigned species **1a** to the peroxo compound $FAlO_2$.[29]

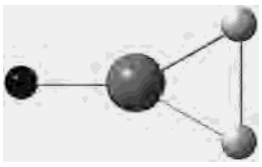

Table 4a includes the calculated wavenumbers and geometry of $FAlO_2$, **1a** (C_{2v} symmetry). $FAlO_2$ has six IR-active vibrational modes spanning the representation $3a_1 + 1b_1 + 2b_2$. The calculations indicate that two of the modes, at 1087.7 and 810.6 cm^{-1} for calculations based on the MP2 method and at 1114.4 and 782.4 cm^{-1} for those based on the B3LYP method, carry sufficient intensity and lie within the range of detection to guarantee their detection in the experiments. The $\nu(^{16}O)/\nu(^{18}O)$ ratios (1.0124 and 1.0141 for MP2 and B3LYP, respectively) are in pleasing agreement with the experimental ratio of 1.0132. The calculations using MP2 and B3LYP methods agree on the wavenumber, but not on the intensity of this vibration, with MP2 predicting a more than 3-fold higher intensity. In both calculations, however, this mode comes fourth in intensity, with the mode at 1087.7 cm^{-1} and two others near 200 cm^{-1} being more intense. The observation of a signal at 781.8 cm^{-1} for species **1a** in the experiments gives further strong support to the assignment of **1a** to the peroxo complex $FAlO_2$. The calculated $\nu(^{16}O)/\nu(^{18}O)$ ratios of 1.0449 and 1.0458 for MP2 and B3LYP, respectively, are in excellent agreement with the observed ratio of 1.0453. Finally, the two modes at 238.2/238.5 and 224.5/217.7 cm^{-1}, exhibiting b_1 and b_2 symmetry, respectively, can be assigned to modes involving out-of-plane deformation and a second torsion. Both modes carry enough intensity for detection, but most probably lie out of the range of detection in our experiments (4000−200 cm^{-1}). The following nonnormalized symmetry coordinates were used in the normal coordinate analysis of all the species of type **1** (X = F, Cl, Br): S_1, r(O−O′); S_2, r(Al−X); S_3, r(Al−O) + r(Al−O′); S_4, γ[X−Al−(μ-O)$_2$]; S_5, r(Al−O) − r(Al−O′); S_6, δ(X−Al−O) − δ(X−Al−O′). Because of the heavy mode coupling, an assignment of the vibrational modes is almost impossible. For $FAlO_2$ the calculations resulted in force constants (N m^{-1}) f(Al−F) = 597.5, f(Al−O) = 444.6, and f(O−O) = 240.7. The value for f(O−O) compares well with the one found for Na_2O_2, where it amounts to 276 N m^{-1}. In contrast the O−O distance for $FAlO_2$ (1.643 Å) is longer than for Na_2O_2 (1.49 Å).[7] The O−O distance is also significantly longer than in complexes to transition-metal centers.[29] On the other hand, the Al−O distance in **1a**−**1c** is surprisingly short and compares well with the ones found in known compounds featuring three-coordinated aluminum such as $CH_3Al(OAr)_2$, where Ar = 2,6-di-*tert*-butyl-4-methylphenyl.[30] This might imply that the O−O distance is elongated to increase the bonding between Al and each of the O atoms. The orbital overlap certainly prefers larger O−Al−O angles. Against this trend operates the force imputed on elongation of the O−O distance, and the O−O distance of 1.66 Å then is the best compromise between these two factors working in opposite directions. All this suggests that the molecule cannot simply be regarded as an ionic complex of O_2^{2-} [although the O−O distance and f(O−O) force constant are close to the values calculated for free O_2^{2-} (1.6258 Å, 197 N m^{-1})] but that the bonding is more difficult to describe, in agreement with the observed heavy coupling

(28) Schnöckel, H.; Mehner, T.; Plitt, H. S.; Schunck, S. *J. Am. Chem. Soc.* **1989**, *111*, 4578. Berkowitz, J. *J. Chem. Phys.* **1958**, *29*, 1386.

(29) Bahlo, J.; Himmel, H.-J.; Schnöckel, H. *Angew. Chem.* **2001**, *113*, 4820; *Angew. Chem. Int. Ed.* **2001**, *40*, 4696.

(30) Haaland, A. In *Coordination Chemistry of Aluminium*; Robinson, G. H., Ed.; VCH: Weinheim, Germany, 1993; p 6 ff.

Table 4. Comparison between the IR Spectra Observed and Calculated [Wavenumbers in cm^{-1}, with Intensities (in km mol^{-1}) in Parentheses] for (a) $FAl(^{16}O_2)/FAl(^{18}O_2)/FAl(^{16}O^{18}O)$, (b) $ClAl(^{16}O_2)/ClAl(^{18}O_2)/ClAl(^{16}O^{18}O)$, and (c) $BrAl(^{16}O_2)/BrAl(^{18}O_2)/BrAl(^{16}O^{18}O)$, **1a**−**1c**

(a) $FAl(^{16}O_2)/FAl(^{18}O_2)/FAl(^{16}O^{18}O)$, **1a**

$FAl(^{16}O_2)$			$FAl(^{18}O_2)$			$FAl(^{16}O^{18}O)$			
	calc[a]			calcd[a]			calcd[a]		
obsd	MP2/TZVPP	B3LYP/6-311G*	obsd	MP2/TZVPP	B3LYP/6-311G*	obsd	MP2/TZVPP	B3LYP/6-3 11G*	assignment
1077.3	1087.7 (147)	1114.4 (144)	1063.6	1074.4 (149)	1098.9 (146)	1070.7	1081.2 (148)	1106.8 (145)	ν_1 (a_1)
c	720.4 (13)	739.8 (14)	c	696.6 (9)	715.7 (9)	c	706.6 (12)	724.0 (12)	ν_2 (a_1)
c	525.6 (12)	528.2 (12)	c	501.6 (12)	504.5 (12)	c	513.9 (12)	516.6 (12)	ν_3 (a_1)
b	238.2 (119)	238.5 (121)	b	236.2 (116)	236.6 (118)	b	237.2 (117)	237.6 (120)	ν_4 (b_1)
781.8	810.6 (66)	782.4 (19)	747.9	775.8 (66)	748.1 (20)	766.8	794.8 (65)	768.8 (19)	ν_5 (b_2)
b	224.5 (74)	217.7 (73)	b	220.6 (70)	213.9 (69	b	222.5 (72)	215.8 (71)	ν_6 (b_2)

(b) $ClAl(^{16}O_2)/ClAl(^{18}O_2)/ClAl(^{16}O^{18}O)$, **1b**

$ClAl(^{16}O_2)$			$ClAl(^{18}O_2)$			$ClAl(^{16}O^{18}O)$			
	calcd[d]			calcd[d]			calcd[d]		
obsd	MP2/TZVPP	B3LYP/6-311G*	obsd	MP2/TZVPP	B3LYP/6-311G*	obsd	MP2/TZVPP	B3LYP/6-311G*	assignment
994.6	993.5 (129)	1016.8 (141)	968.3	969.8 (133)	990.5 (145)	982.1	982.5 (131)	1004.3 (143)	ν_1 (a_1)
549.3	597.9 (52)	608.8 (59)	518.5	571.7 (45)	582.8 (52)	c	584.8 (48)	595.8 (55)	ν_2 (a_1)
c	435.1 (1)	431.7 (1)	c	423.1 (0.1)	420.1 (1)	c	429.2 (0.4)	426.0 (1)	ν_3 (a_1)
b	200.1 (79)	196.9 (85)	b	197.9 (76)	194.7 (83)	b	198.0 (78)	195.8 (84)	ν_4 (b_1)
778.7	803.7 (51)	771.1 (14)	745.0	768.8 (50)	737.1 (15)	761.0	785.6 (51)	753.6 (15)	ν_5 (b_2)
b	179.6 (45)	176.5 (47)	b	175.6 (42)	172.6 (44)	b	177.5 (43)	174.5 (46)	ν_6 (b_2)

(c) $BrAl(^{16}O_2)/BrAl(^{18}O_2)/BrAl(^{16}O^{18}O)$, **1c**

$BrAl(^{16}O_2)$			$BrAl(^{18}O_2)$			$BrAl(^{16}O^{18}O)$			
	calcd[e]			calcd[e]			calcd[e]		
obsd	MP2/TZVPP	B3LYP/6-311G*	obsd	MP2/TZVPP	B3LYP/6-311G*	obsd	MP2/TZVPP	B3LYP/6-311G*	assignment
972.4	976.0 (120)	998.9 (128)	946.9	950.2 (123)	970.9 (131)	960.7	964.2 (121)	985.8 (129)	ν_1 (a_1)
524.2	582.1 (52)	592.8 (55)	500.8	554.2 (45)	565.0 (48)	512.1	568.3 (48)	579.1 (52)	ν_2 (a_1)
c	335.2 (3)	332.0 (3)	c	326.1 (2)	323.1 (2)	c	330.7 (2)	327.6 ()	ν_3 (a_1)
b	191.0 (68)	184.3 (73)	b	188.7 (66)	182.0 (71)	b	189.8 (67)	183.1 (71)	ν_4 (b_1)
774.0	800.2 (46)	764.5 (13)	741.0	765.3 (46)	730.7 (13)	756.3	781.8 (47)	746.8 (14)	ν_5 (b_2)
b	166.8 (38)	163.9 (40)	b	162.6 (35)	159.9 (37)	b	164.6 (36)	161.9 (38)	ν_6 (b_2)

[a] C_{2v} symmetry. Geometry (bond lengths in angstroms, angles in degrees): (MP2/TZVPP) Al−F 1.6430, Al−O 1.7006, O−O 1.6596, O−Al−O 58.4; (B3LYP/6-311G*) Al−F 1.6390, Al−O 1.7102, O−O 1.6637, O−Al−O 58.4. [b] Out of range of detection. [c] Too weak to be detected. [d] C_{2v} symmetry. Geometry (bond lengths in angstroms, angles in degrees): (MP2/TZVPP) Al−Cl 2.0556, Al−O 1.7051, O−O 1.6532, O−Al−O 58.0; (B3LYP/6-311G*) Al−Cl 2.0593, Al−O 1.7117, O−O 1.6592, O−Al−O 58.0. [e] C_{2v} symmetry. Geometry (bond lengths in angstroms, angles in degrees): (MP2/TZVPP) Al−Br 2.2081, 1.7079, O−O 1.6510, O−Al−O 57.8; (B3LYP/6-311G*) Al−Br 2.2114, Al−O 1.7130, O−O 1.6576, O−Al−O 57.9.

of the vibrational modes. The strong interaction between Al and O in the compound expresses itself also in the surprisingly low energy difference to the triplet electronic states, in which the O−O distance is significantly elongated (2.30 Å; see below).

Species **1b**, the Cl-equivalent of **1a**, again contains two equivalent O atoms. Table 4b includes the observed and calculated wavenumbers of $ClAlO_2$ for all relevant isotopomers. Our experiments hit on three of the six vibrations. The mode with the calculated wavenumbers of 993.5 and 1016.8 cm^{-1} for MP2 and B3LYP, respectively, can again be assigned to the a_1 mode, whose wavenumber fits well to the observed value of 994.6 cm^{-1}. This assignment is confirmed by the calculated $\nu(^{16}O)/\nu(^{18}O)$ ratios of 1.0244 and 1.0266 for MP2 and B3LYP, respectively, and the experimental value of 1.0272:1. Next in the order of decreasing wavenumber comes a b_2 mode at 803.7 and 771.1 cm^{-1} for MP2 and B3LYP, respectively. This mode is only slightly affected by replacement of F by Cl. As with $FAlO_2$, the ab initio and DFT methods disagree on the intensity of the corresponding IR absorption. However, the calculated wavenumbers are again in excellent agreement with the experimental value of 778.7 cm^{-1}, and so are the $\nu(^{16}O)/\nu(^{18}O)$ ratios (1.0454:1/1.0461:1 calculated with MP2/B3LYP vs 1.0432:1 found in the experiments). The signal observed at 549.3 cm^{-1} compares with the calculated value of 597.9/608.8 cm^{-1} for MP2/B3LYP calculations. Experimental and calculated (MP2/B3LYP) $\nu(^{16}O)/\nu(^{18}O)$ ratios are 1.0594:1 and 1.0458:1/1.0446:1, respectively. The force constants amount to (N m^{-1}) $f(Al-Cl) = 272.4$, $f(Al-O) = 456.6$, and $f(O-O) = 173.3$.

Our experiments identify three of the six vibrations of singlet $BrAlO_2$, **1c**. The highest a_1 mode follows the trend toward lower wavenumbers from F to Cl and again to Br. The calculated wavenumbers of 976.0 and 998.9 cm^{-1} for MP2 and B3LYP, respectively, are in line with the experimental value of 972.4 cm^{-1}. Again, the comparison between the calculated $\nu(^{16}O)/\nu(^{18}O)$ ratio (1.0272/1.0288 with MP2/B3LYP) and the observed one (1.0269) fulfills all expectations. Next comes the b_2 mode, which shows but minor changes in wavenumber for all three $XAlO_2$ species. With calculated wavenumbers of 800.2 and 764.5 cm^{-1} for MP2 and B3LYP, the experimental value of 774.0 cm^{-1} is very close to the calculated one, and yet again the agreement between the $\nu(^{16}O)/\nu(^{18}O)$ ratios calculated (1.0456/1.0463 for MP2 and B3LYP) and observed (1.0452) leaves little

Table 5. Comparison of the Geometries of Compounds **1a**−**1c** with Other Known Species Bearing the Formula MO_2 and with Two Equivalent O Atoms as Well as O_2, O_2^-, O_2^{2-} (Distances in Angstroms, Angles in Degrees)

compound	r(O−O)	r(M−O)	∠(O−M−O)	ref
MgO_2 singlet[b]	1.6608	1.8298	63.1	calcd[a]
MgO_2 triplet[b]	1.3564	2.0174	70.3	calcd[a]
$(Ph_3P)_2PtO_2$	1.26	1.99/1.90	38	27
{Cu[HB(3,5-^{i}Pr$_2$pz)$_3$]}$_2$(O_2)[c]	1.412	1.903/1.927	43.3	28
AlO_2	1.6394	1.7296	61.7	calcd[a]
$FAlO_2$	1.6596	1.7006	58.4	calcd[a]
$ClAlO_2$	1.6532	1.7051	58.0	calcd[a]
$BrAlO_2$	1.6510	1.7079	57.8	calcd[a]
GaO_2	1.6414	1.8267	63.3	calcd[a]
$OSiO_2$	1.65	1.63[d]	60.7	6
F_2SiO_2	1.6458	1.6266	60.8	calcd[a]
O_2	1.2055			calcd[a]
O_2^-	1.3519			calcd[a]
O_2^{2-}	1.6258			calcd[a]

[a] B3LYP/6-311G*. [b] ΔE(singlet−triplet) = −123 kJ mol^{-1} (the first singlet electronic state is 123 kJ mol^{-1} higher in energy than the triplet electronic ground state). [c] pz = pyrazolyl. [d] Distance between Si and O of the peroxo group.

room for doubt. However, the experimentally observed relative intensity of this absorption is in good agreement with that predicted by MP2, but not with that predicted by B3LYP calculations. Thus, it appears that B3LYP has consistently the same problem in predicting the intensity of this mode for all three peroxo species $XAlO_2$ (X = F, Cl, and Br). The wavenumber of the third absorption, at 524.2 cm^{-1} in our experiments, compares with the values of 582.1 and 592.8 cm^{-1} expected on the basis of MP2 and B3LYP, respectively. The experimental $\nu(^{16}O)/\nu(^{18}O)$ ratio of 1.0467 compares with the calculated one of 1.0503/1.0492 with MP2/B3LYP. The normal coordinate analysis gave the following values (force constants in N m^{-1}): f(Al−Br) = 255.1; f(Al−O) = 431.6; f(O−O) = 140.4. The trend in the wavenumbers upon replacement of X is that the largest changes happen for the step from X = F to X = Cl. The following step from X = Cl to X = Br leads to only minor changes. The decrease of the force constant f(O−O) reflects the change of the partial charge on the O_2 group, which rises from $FAlO_2$ to $BrAlO_2$.

The characterization of these three new peroxo species invites comparison with similar species. Table 5 compares the geometries of **1a**−**1c** with those of other known O_2 complexes with two equivalent O atoms. It also includes the results of calculations on O_2, O_2^-, and O_2^{2-} at the given level of theory. The group 1 atoms form ionic MO_2 complexes with C_{2v} symmetry. The wavenumber of the O−O stretching fundamental is very close to that observed for free O_2^-. The experimental and quantum chemical studies for MgO_2 yield a rather unexpected result, since they favor a triplet electronic ground state with an O−O bond length close to that of O_2^- instead of a singlet state, which would be closer to the formulation $Mg^{2+}O_2^{2-}$. Geometry constraints might be one of the major factors at work here. On the other hand, Al and Ga form O_2 complexes with O−O bond lengths close to the value expected for O_2^{2-}. The $XAlO_2$ complexes exhibit geometries close to those of $OSiO_2$ and F_2SiO_2. The table also includes the geometries of the two transition-metal complexes $(Ph_3P)_2PtO_2$[31] and {Cu[HB(3,5-^{i}Pr$_2$pz)$_3$]}$_2$(O_2).[32] The latter is a dinuclear complex and serves as a model system for oxyhemocyanin, as already mentioned above. Both are slightly distorted with two nonequivalent M−O distances. The Pt complex exhibits an O−O bond length which is between those of O_2 and O_2^-. In the dinuclear Cu complex the O−O bond length is longer than for O_2^-, but shorter than for O_2^{2-} and the $XAlO_2$ complexes.

$XAl(\mu\text{-}O)_2AlX$, 2a−2c. Calculations on $XAl(\mu\text{-}O)_2AlX$ (X = F, Cl, and Br) give a planar D_{2h} structure with the following distances (Å) (X = F, Cl, and Br, respectively): Al−X 1.6516/2.0720/2.2285; Al−O 1.7461/1.7486/1.7509; Al−Al 2.5457/2.5389/2.5401. The O−Al−O angles were calculated to be 93.6°, 93.1°, and 93.0 for X = F, Cl, and Br, respectively. The Al−O and Al−Al distances are therefore somewhat shorter than those found in crystals of known compounds with $Al(\mu\text{-}O)_2Al$ ring structures[33] [e.g., Al−O 1.810 Å and Al−Al 2.7527 Å for $H_2Al(\mu\text{-}O^t\text{-}Bu)_2AlH_2$].

The wavenumber calculations give the following values for $FAl(\mu\text{-}O)_2AlF$ [cm^{-1}, with symmetry labeling and intensities (km mol^{-1}) in parentheses] (Table 6a): 1015.0 (0, a_g), 960.0 (516, b_{1u}), 819.2 (279, b_{2u}), 739.4 (0, a_g), 671.9 (0, b_{3g}), 652.2 (36, b_{1u}), 393.5 (0, a_g), 388.5 (187, b_{3u}), 226.7 (0, b_{3g}), 220.0 (0, b_{2g}), 162.9 (32, b_{2u}), 91.0 (11, b_{3u}). Thus, the spectrum should be dominated by the two strong absorptions at 960.0 and 819.2 cm^{-1}.

It has been mentioned above that the signal at 1077.3 cm^{-1} of species **1a** has previously been assigned to $FAl(\mu\text{-}O)_2AlF$.[16] However, the deviation between the experimental and calculated wavenumbers for this mode would then be more than 10%. Further support for the identification of **1a** as the peroxo species $FAlO_2$ and not $FAl(\mu\text{-}O)_2AlF$ comes from comparison of the ^{18}O shift. The calculated shift for $FAl(\mu\text{-}^{18}O)_2AlF$ is as small as 4.8 cm^{-1} (wavenumber of 1010.2 cm^{-1}). In the experiments, however, we have observed a shift of 13.7 cm^{-1}. Thus, **1a** is in all certainty the peroxo species $FAlO_2$. On the other hand, the signals due to species **2a** are in pleasing agreement with what is expected for $FAl(\mu\text{-}O)_2AlF$ on the basis of our calculations. Thus, the signals at 942.8 and 812.9 cm^{-1} in our experiments can be assigned to the b_{1u} and b_{2u} modes, respectively, of $FAl(\mu\text{-}O)_2AlF$. The observed $\nu(^{16}O)/\nu(^{18}O)$ ratios of 1.0070 and 1.0348 match almost perfectly the calculated ones of 1.0070 and 1.0351 (B3LYP), respectively.

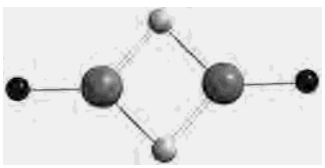

For $ClAl(\mu\text{-}O)_2AlCl$ we have calculated wavenumbers [cm^{-1}, with symmetry labeling and intensities (km mol^{-1})

(31) Cook, C. D.; Cheng, P.-T.; Nyburg, S. C. *J. Am. Chem. Soc.* **1969**, *91*, 2123.
(32) Kitajima, N.; Fujisawa, K.; Fujimoto, C.; Moro-oka, Y.; Hashimoto, S.; Kitagawa, T.; Toriumi, K.; Tatsumi, K.; Nakamura, A. *J. Am. Chem. Soc.* **1992**, *114*, 1277−1291.

Table 6. Comparison between the IR Spectra Observed and Calculated [Wavenumbers in cm^{-1}, with Intensities (in km mol^{-1}) in Parentheses] for (a) FAl(μ-^{16}O)$_2$AlF, FAl(μ-^{18}O)$_2$AlF, and FAl(μ-^{16}O^{18}O)AlF, **2a**, (b) ClAl(μ-^{16}O)$_2$AlCl, ClAl(μ-^{18}O)$_2$AlCl, and ClAl(μ-^{16}O^{18}O)AlCl, **2b**, and (c) BrAl(μ-^{16}O)$_2$AlBr, BrAl(μ-^{18}O)$_2$AlBr, and BrAl(μ-^{16}O^{18}O)AlBr, **2c**

(a) FAl(μ-^{16}O)$_2$AlF, FAl(μ-^{18}O)$_2$AlF, and FAl(μ-^{16}O^{18}O)AlF, **2a**

FAl(μ-^{16}O)$_2$AlF		FAl(μ-^{18}O)$_2$AlF		FAl(μ-^{16}O^{18}O)AlF		
obsd	calcd[a] (B3LYP/6-311G*)	obsd	calcd[a] (B3LYP/6-311G*)	obsd	calcd[a] (B3LYP/6-311G*)	assignment
c	1015.0 (0)	c	1010.2 (0)	c	1012.6 (0.3)	ν_1 (a_g)
c	739.4 (0)	c	703.5 (0)	c	718.8 (8)	ν_2 (a_g)
c	393.5 (0)	c	391.7 (0)	c	392.6 (0.01)	ν_3 (a_g)
942.8	960.0 (516)	936.2	953.3 (493)	939.4	956.7 (504)	ν_4 (b_{1u})
c	652.2 (0)	c	629.1 (41)	c	634.9 (32)	ν_5 (b_{1u})
b	220.0 (0)	b	220.0 (0)	b	220.0 (0)	ν_6 (b_{2g})
812.9	819.2 (279)	785.6	791.4 (267)	802.7	808.0 (265)	ν_7 (b_{2u})
b	162.9 (32)	b	161.5 (31)	b	162.2 (32)	ν_8 (b_{2u})
c	671.9 (0)	c	646.9 (0)	c	665.1 (6)	ν_9 (b_{3g})
b	226.7 (0)	b	223.6 (0)	b	225.1 (0.001)	ν_{10} (b_{3g})
b	91.0 (11)	b	89.7 (11)	b	90.4 (11)	ν_{11} (b_{3u})

(b) ClAl(μ-^{16}O)$_2$AlCl, ClAl(μ-^{18}O)$_2$AlCl, and ClAl(μ-^{16}O^{18}O)AlCl, **2b**

ClAl(μ-^{16}O)$_2$AlCl		ClAl(μ-^{18}O)$_2$AlCl		ClAl(μ-^{16}O^{18}O)AlCl		
obsd	calcd[d] (B3LYP/6-311G*)	obsd	calcd[d] (B3LYP/6-311G*)	obsd	calcd[d] (B3LYP/6-311G*)	assignment
c	870.8 (0)	c	851.3 (0)	c	862.6 (7)	ν_1 (a_g)
c	649.1 (0)	c	626.6 (0)	c	637.4 (1)	ν_2 (a_g)
b	286.8 (0)	b	286.5 (0)	b	286.7 (0.001)	ν_3 (a_g)
809.8	809.2 (749	788.5	789.0 (726)	800.3	799.9 (734)	ν_4 (b_{1u})
c	471.9 (16)	c	462.0 (11)	c	466.8 (13)	ν_5 (b_{1u})
b	184.9 (0)	b	184.9 (0)	b	184.9 (0)	ν_6 (b_{2g})
804.7	807.5 (217)	777.1	779.6 (206)	790.3	792.5 (204)	ν_7 (b_{2u})
b	101.9 (9)	b	100.7 (9)	b	101.3 (9)	ν_8 (b_{2u})
c	667.0 (0)	c	642.4 (0)	c	654.1 (4)	ν_9 (b_{3g})
b	180.7 (0)	b	177.5 (0)	b	179.1 (0.003)	ν_{10} (b_{3g})
b	59.4 (4)	b	58.5 (4)	b	58.9 (4)	ν_{11} (b_{3u})

(c) BrAl(μ-^{16}O)$_2$AlBr, BrAl(μ-^{18}O)$_2$AlBr, and BrAl(μ-^{16}O^{18}O)AlBr, **2c**

BrAl(μ-^{16}O)$_2$AlBr		BrAl(μ-^{18}O)$_2$AlBr		BrAl(μ-^{16}O^{18}O)AlBr		
obsd	calcd[e] (B3LYP/6-311G*)	obsd	calcd[e] (B3LYP/6-311G*)	obsd	calcd[e] (B3LYP/6-311G*)	assignment
c	849.6 (0)	c	826.0 (0)	c	840.5 (11)	ν_1 (a_g)
c	615.3 (0)	c	596.7 (0)	c	605.8 (0.4)	ν_2 (a_g)
b	187.0 (0)	b	187.0 (0)	b	187.0 (0)	ν_3 (a_g)
790.2	788.5 (766)	763.1	765.9 (736)	780.4	778.2 (746)	ν_4 (b_{1u})
b	365.2 (17)	b	354.6 (105)	b	360.3 (108)	ν_5 (b_{1u})
b	169.1 (0)	b	169.1 (0)	b	169.1 (0.001)	ν_6 (b_{2g})
800.9	800.7 (193)	774.7	773.0 (182)	c	784.4 (175)	ν_7 (b_{2u})
b	78.4 (3)	b	77.2 (3)	b	77.8 (3)	ν_8 (b_{2u})
c	662.0 (0)	c	637.6 (0)	c	648.9 (5)	ν_9 (b_{3g})
b	165.7 (0)	b	162.4 (0)	b	164.0 (0.001)	ν_{10} (b_{3g})
b	45.9 (2)	b	45.0 (2)	b	45.5 (2)	ν_{11} (b_{3u})

[a] D_{2h} symmetry. Geometry (bond lengths in anstroms, angles in degrees): (B3LYP/6-311G*) Al−F 1.6516, Al−O 1.7461, Al−Al 2.5457, O−Al−O 93.6. [b] Out of range of detection. [c] Too weak to be detected. [d] D_{2h} symmetry. Geometry (bond lengths in anstroms, angles in degrees): (B3LYP/6-311G*) Al−Cl 2.0720, Al−O 1.7486, Al−Al 2.5389, O−Al−O 93.1. [e] D_{2h} symmetry. Geometry (bond lengths in anstroms, angles in degrees): (B3LYP/6-311G*) Al−Br 2.2285, Al−O 1.7509, Al−Al 2.5401, O−Al−O 93.0.

in parentheses] (Table 6b) of 870.8 (0, a_g), 809.2 (749, b_{1u}), 807.5 (217, b_{2u}), 667.0 (0, a_g), 649.1 (0, b_{3g}), 471.9 (16, b_{1u}), 371.5 (131, b_{3u}), 286.8 (0, a_g), 184.9 (0, b_{2g}), 180.7 (0, b_{3g}), 101.9 (9, b_{2u}), and 59.4 (4, b_{3u}). Thus, two modes have wavenumbers (at 809.2 and 807.5 cm^{-1}) as well as IR intensities which should guarantee their detection in our experiments, subject to the formation of the molecule in sufficient yields. Species **1b** gave evidence for three absorptions located at 994.6, 778.7, and 549.3 cm^{-1}. The observation of a signal at 549.3 cm^{-1} due to **1b** excludes ClAl(μ-O)$_2$AlCl from being the author of this observed absorption. The signals at 809.8 and 790.3 cm^{-1} of species **2b** observed in our experiments are, however, in very good agreement with the properties calculated for ClAl(μ-O)$_2$AlCl. Thus, the two signals can be assigned to the two modes predicted to be most intense in IR absorption for this species, i.e., the b_{1u} and b_{2u} modes near 800 cm^{-1}. The $\nu(^{16}O)/\nu(^{18}O)$ ratios lent further support to this assignment (calculated, 1.0256 and 1.0358; experimental, 1.0270 and 1.0355).

(33) Veith, M.; Faber, S.; Wolfanger, H.; Huch, V. *Chem. Ber.* **1996**, *129*, 381. Uhl, W.; Gerding, R.; Vester, A. *J. Organomet. Chem.* **1996**, *513*, 163. Benn, R.; Rufiñska, A.; Lehmkühl, H.; Janssen, E.; Krüger, C. *Angew. Chem.* **1983**, *95*, 808; *Angew. Chem., Int. Ed. Engl.* **1983**, *22*, 779. Veith, M.; Jarczyk, M.; Huch, V. *Angew. Chem.* **1997**, *109*, 140; *Angew. Chem., Int. Ed. Engl.* **1997**, *36*, 117. Boker, C.; Noltemeyer, M.; Gornitzka, H.; Kneisel, B. O.; Teichert, M.; Herbst-Irmer, R.; Meller. A. *Main Group Met. Chem.* **1998**, *21*, 565.

Finally, the calculations for BrAl(μ-O)$_2$AlBr yield the following wavenumbers [cm^{-1}, with symmetry labeling and intensities (km mol^{-1}) in parentheses] (Table 6c): 849.6 (0, a_g), 800.7 (193, b_{2u}), 788.5 (766, b_{1u}), 662.0 (0, b_{3g}), 615.3 (0, a_g), 366.0 (111, b_{3u}), 365.2 (17, b_{1u}), 187.0 (0, a_g), 169.1 (0, b_{2g}), 165.7 (0, b_{3g}), 78.4 (3, b_{2u}), 45.9 (2, b_{3u}). That this species cannot be assigned to **1c** is again evidenced by the detection of an absorption at 524.2 cm^{-1} due to **1c**. We can identify species **2c**, however, as BrAl(μ-O)$_2$AlBr. The signals at 800.9 and 790.2 cm^{-1} can thus be assigned to the high-wavenumber b_{2u} and b_{1u} modes, respectively, for this absorber.

Triplet XAlO$_2$. According to our calculations, the electronic ground state of XAlO$_2$ (X = F, Cl, and Br) is a singlet. The O−O force constant calculated on the basis of the experimental results indicates the presence of an intact O−O bond, although the O−O interaction is, as expected, reduced with respect to free dioxygen. This corresponds to the observations made for Na_2O_2 [f(O−O) = 276 N m^{-1}].[7] However, the energy gap to the first triplet state, also with C_{2v} symmetry, is calculated to be only 38.2, 38.6, and 39.6 kJ mol^{-1} for X = F, Cl, and Br, respectively. With values of 2.2990, 2.2913, and 2.2892 Å, the O−O distances are, as expected, much longer than those of the molecules in their singlet ground states (1.6596, 1.6532, and 1.6510 Å). Accordingly, the mode assigned to the O−O stretching fundamental is calculated to have wavenumbers as low as 240.1, 235.6, and 223.2 cm^{-1} for X = F, Cl, and Br, respectively. With the increasing O−O distance comes an increase of the O−Al−O angle from 58.4°, 58.0°, and 57.8° in the singlet states to 84.2°, 83.6°, and 83.4° in the triplet states, for X = F, Cl, and Br, respectively. Other geometrical parameters, namely, the Al−X and Al−O distances, undergo only small changes with the switch from singlet to triplet. The Al−X distances of 1.6430, 2.0556, and 2.2081 Å and the Al−O distances of 1.7006, 1.7051, and 1.7079 Å for X = F, Cl, and Br, respectively, in the singlet state compare with values of 1.6497, 2.0691, and 2.2220 Å for the Al−X distances and 1.7139, 1.7173, and 1.7200 Å for the Al−O distances in the molecules in their triplet states.

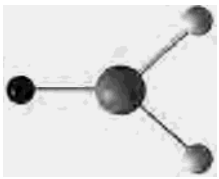

The following wavenumbers [cm^{-1}, with intensities (km mol^{-1}) and symmetry assignments in parentheses] were calculated: 1041.3 (144, a_1), 793.6 (15, b_2), 690.3 (3, a_1), 240.1 (14, a_1), 233.0 (105, b_1), and 196.7 (28, b_2) for FAlO$_2$; 928.9 (149, a_1), 793.5 (15, b_2), 479.9 (36, a_1), 235.6 (12, a_1), 198.2 (4, b_1), and 155.1 (17, b_2) for ClAlO$_2$; 910.7 (136, a_1), 789.4 (15, b_2), 382.1 (35, a_1), 223.2 (8, a_1), 186.5 (63, b_1), and 144.1 (13, b_2) for BrAlO$_2$. The signals at 1042.3, 957.4/953.4, and 897.8 cm^{-1} (X = F, Cl, Br) in our experiments occur at wavenumbers in good agreement with those calculated for the most intense IR fundamental of each molecule. The $\nu(^{16}O)/\nu(^{18}O)$ ratios observed (1.01519/1.03705/1.03350) and calculated (1.01205/1.02675/1.02927) lend further support to assigning the observed signals to the species XAlO$_2$ in their *triplet* states. It is clear from a comparison of the calculated and observed intensities that only a small fraction of XAlO$_2$ molecules are in the triplet state, as opposed to the singlet state of **1a**−**1c**.

Singlet XAlOO. There was no evidence that this species is formed in significant yields in our experiments. Nevertheless, its structure and vibrational properties were calculated. These calculations converged to a minimum only for the molecule in the electronic singlet state; the triplet state seems to be unstable to distortion in the direction of the structure with two equivalent O atoms (triplet XAlO$_2$). The O−O distances for the singlet superoxides are, as expected, much reduced in comparison with the peroxide structures. We found values of 1.3218, 1.2967, and 1.2990 Å for X = F, Cl, and Br, respectively. The Al−O−O and X−Al−O angles amount to 132.5° and 141.1°, 144.8° and 115.1°, and 145.4° and 116.0° for X = F, Cl, and Br, respectively. Finally, the corresponding Al−X and Al−O distances (Å) were found to be 1.6694 and 1.7837, 2.1142 and 1.7603, and 2.2750 and 1.7549 for X = F, Cl, and Br.

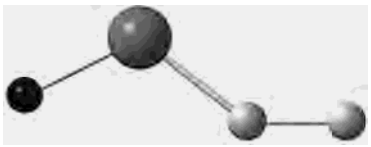

The following wavenumbers (cm^{-1}) were calculated [with intensities (km mol^{-1}) in parentheses]: 1121.9 (327, a′), 834.4 (123, a′), 462.7 (12, a′), 331.9 (9, a′), 142.6 (9), and 88.7 (4) for FAlOO; 1186.7 (363, a′), 602.9 (69, a′), 441.9 (98, a′), 332.6 (4, a′), 119.3 (1), and 107.8 (10) for ClAlOO; 1178.7 (370, a′), 583.2 (25, a′), 387.6 (108, a′), 301.5 (5, a′), 119.0 (1), and 90.5 (9) for BrAlOO. The three modes with the highest wavenumbers can be assigned in each case to the O−O, Al−F, and Al−O stretching fundamentals. Mode-coupling is reduced with respect to the situation in the peroxide complexes.

We continue our survey with the investigation of additional possible products of the reaction of (AlX)$_2$, namely, the peroxo complexes Al(μ-X)$_2$AlO$_2$ and XAlOOAlX, although the experiments gave no indication for the formation of either of these.

Al(μ-X)$_2$AlO$_2$. As expected, this species exhibits C_{2v} symmetry, with the Al−O$_2$− plane being perpendicular to the Al(μ-X)$_2$Al plane. We anticipate the geometry of the peroxo complex to be similar to that of the XAlO$_2$ species. Thus, the O−O distances and O−Al−O angles are 1.6467 Å and 61.2° for X = F, 1.6380 Å and 61.5° for X = Cl, and 1.6349 Å and 56.7° for X = Br. Other geometrical parameters (distances in angstroms, angles in degrees) are Al−X 1.7870, 2.2218, and 2.3810, Al−Al 2.6932, 3.4942, and 3.6338, and X−Al−X (the first value is the angle of the Al that is engaged in the O$_2$ complex)

82.2/72.0, 95.1/78.8, and 98.0/81.9, for X = F, Cl, and Br, respectively.

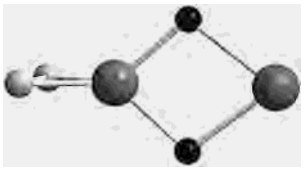

The following wavenumbers in (cm^{-1}, with intensities (km mol^{-1}) and symmetry assignments in parentheses] were calculated: 1012.2 (202, a_1), 766.2 (16, b_1), 632.0 (74, a_1), 560.9 (76, b_2), 526.9 (2, a_1), 406.8 (232, a_1), 301.6 (67, b_2), 298.6 (14, a_1), 265.7 (40, b_1), 130.9 (9, b_2), 111.7 (0, a_2), and 85.5 (5, b_1) for Al(μ-F)$_2$AlO$_2$; 963.6 (151, a_1), 750.5 (12, b_1), 583.8 (60, a_1), 402.4 (120, b_2), 346.0 (16, a_1), 242.2 (151, a_1), 195.9 (31, b_1), 191.4 (46, b_2), 177.6 (3, a_1), 100.3 (0, a_2), 93.5 (0.02, b_2), and 45.9 (0.2, b_1) for Al(μ-Cl)$_2$AlO$_2$; 952.2 (137, a_1), 743.0 (11, b_1), 581.8 (55, a_1), 337.7 (113, b_2), 248.0 (7, a_1), 212.0 (99, a_1), 176.4 (24, b_1), 151.7 (30, b_2), 123.1 (0.3, a_1), 97.8 (0, a_2), 94.4 (0.3, b_2), and 34.2 (0.1, b_1) for Al(μ-Br)$_2$AlO$_2$.

XAlOOAlX. The calculations predict a planar geometry (C_{2v} symmetry) for all three molecules of this type. Thus, the structure differs from that of H_2O_2, where a dihedral angle of 111.5° is found for the molecule in the gas phase.[7] Thus, there appears to be an Al−Al interaction which overcompensates the barrier to rotation of 29.45 kJ mol^{-1} in H_2O_2.[34] This interaction manifests itself also in a reduced Al−Al distance (2.4497, 2.4701, and 2.4771 for X = F, Cl, and Br, respectively). With 1.4944, 1.4930, and 1.4927 Å for X = F, Cl, and Br, respectively, the O−O distances are in good agreement with the value observed for H_2O_2 (1.475 Å). Other geometrical parameters are the Al−O and Al−X distances (Å) of 1.7645 and 1.6619 for X = F, 1.7656 and 2.0943 for X = Cl, and 1.7674 and 2.2523 for X = Br. Finally, the X−Al−O and Al−O−O angles were calculated to be 125.0° and 105.7° for X = F, 123.9° and 106.1° for X = Cl, and 124.2° and 106.2° for X = Br.

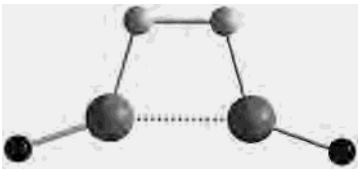

Our wavenumber analysis gave the following values for XAl^{16}O^{16}OAlX [cm^{-1}, with intensity (km mol^{-1}) and symmetry assignments in parentheses]: 963.4 (51, a_1), 881.2 (252, b_2), 868.6 (1, a_1), 690.9 (99, a_1), 666.1 (25, b_2), 338.1 (20, a_1), 306.4 (32, b_2), 204.9 (0, a_2), 192.3 (23, b_2), 135.2 (16, a_1), 120.3 (53, b_1), and 114.8 (0, a_2) for X = F; 882.0 (22, a_1), 747.7 (92, a_1), 724.8 (83, b_2), 597.4 (16, a_1), 511.7 (309, b_2), 289.7 (14, b_2), 252.8 (10, a_1), 184.9 (0, a_2), 151.8 (20, b_2), 112.2 (0, a_2), 89.5 (32, b_1), and 84.9 (5, a_1) for X = Cl; 878.4 (17, a_1), 732.3 (92, a_1), 713.3 (48, b_2), 544.9 (9, a_1), 434.7 (307, b_2), 258.7 (1, b_2), 179.9 (5, a_1), 175.8 (0, a_2), 137.4 (17, b_2), 105.1 (0, a_2), 74.6 (24, b_1), and 60.9 (2, a_1) for X = Br. It is no surprise that the ν(O−O) fundamental comes at a higher wavenumber (868.6, 882.0, and 878.4 cm^{-1} for F, Cl, and Br, respectively) than in the μ-η^2-O_2 complexes, but at a lower wavenumber than in the superoxo complex XAlOO, in line with the relevant O−O bond distances.

Reaction Pathways. No product of a spontaneous reaction of AlX with O_2 was detected in the IR spectra taken upon co-deposition. Photolysis is needed to initiate the reaction. Hence, the reaction with O_2 follows the pattern observed for other reactions of AlX and its higher homologues GaX and InX, e.g., with H_2 or HX.[35,36] Our experiments have identified the peroxo complex $XAlO_2$ as the main product of the reaction with one O_2 molecule. A small percentage of this species was found to be not in the singlet electronic ground state, but in the triplet state. This triplet state is higher in energy than the singlet ground state by only 38.2, 38.6, and 39.6 kJ mol^{-1} (for X = F, Cl, and Br, respectively).

Reaction A1, leading to singlet $XAlO_2$, is exothermic with reaction energies calculated to be −140.3, −149.8, and −153.4 kJ mol^{-1} for X = F, Cl, and Br, respectively.

The corresponding reaction of $(AlX)_2$ to give the peroxo complex (reaction A2) is also exothermic with energies of −213.2, −204.5, and −200.3 kJ mol^{-1} for X = F, Cl, and Br, respectively.

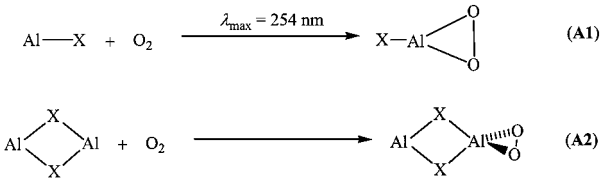

An *end-on* approach of the dioxygen molecule to AlX should lead first to the superoxide species XAlOO (reaction B1). By analogy, $(AlX)_2$ should form the superoxide Al(μ-X)$_2$AlOO (reaction B2). The formation of XAlOO is endothermic, the calculated energies being 79.4, 66.2, and 60.9 kJ mol^{-1} (X = F, Cl, and Br, respectively, reaction B1). We failed to find an energy minimum structure for Al(μ-X)-AlOO, the corresponding product of the reaction of the $(AlX)_2$ dimer. All attempts resulted in a structure with at least one imaginary vibrational wavenumber.

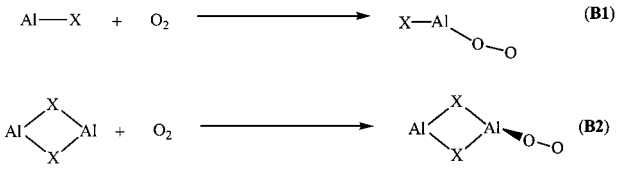

The peroxide and the superoxide are the only products of the reaction with Al−X monomers that include Al−O bonds and have the formula $XAlO_2$. The reaction with $(AlX)_2$ can

(34) Savariault, J.-M.; Lehmann, M. S. *J. Am. Chem. Soc.* **1980**, *102*, 1298.

(35) Köppe, R.; Tacke, M.; Schnöckel, H. *Z. Anorg. Allg. Chem.* **1991**, *605*, 35. Köppe, R.; Schnöckel, H. *J. Chem. Soc., Dalton Trans.* **1992**, 3393.

(36) Himmel, H.-J.; Downs, A. J.; Greene, T. M. *J. Am. Chem. Soc.* **2000**, *122*, 922.

lead to two more products, namely, $XAl(\mu\text{-}O)_2AlX$, now with two O atoms in bridging positions, and the peroxide-like species XAlOOAlX. The formation of $XAl(\mu\text{-}O)_2AlX$ (reaction C) proceeds with energies of −748.4, −821.6, and −813.6 kJ mol^{-1} for X = F, Cl, and Br, respectively. Less energetic is the formation of XAlOOAlX with energies of −308.9, −315.3, and −318.7 kJ mol^{-1} (reaction D) for X = F, Cl, and Br, respectively. Hence, $XAl(\mu\text{-}O)_2AlX$ represents the lowest energy structure of the possible species with the formula $X_2Al_2O_2$. It is not surprising therefore that our experiments find evidence only for this species as the product of the reaction of the dimer $(AlX)_2$. The mechanism of formation may include the generation of the peroxo species $Al(\mu\text{-}X)_2AlO_2$ as an intermediate.

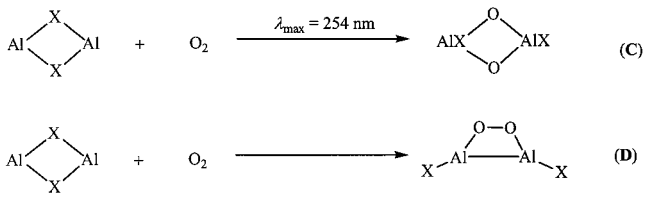

Conclusions

The photolytically induced reactions of AlX monomers (X = F, Cl, or Br) with O_2 were shown to give the peroxo species $XAlO_2$, all with C_{2v} symmetry. The majority of $XAlO_2$ molecules were found to be in their singlet electronic ground states, but small quantities of what may well be triplet-state $XAlO_2$ molecules were also present. According to our DFT calculations, the singlet−triplet gap amounts to about 40 kJ mol^{-1} for all species. The experimental data together with the calculated ones give insight into the structure and bonding of these molecules, which exhibit surprisingly large O−O distances of ca. 1.65 Å in the singlet electronic state and ca. 2.30 Å in the triplet electronic state. The reactions of the dimer $(AlX)_2$ yield the species $XAl(\mu\text{-}O)_2AlX$. This species is the lowest energy form of all the isomers with the formula $X_2Al_2O_2$. Though the Al−Al distance is less than 2.26 Å, an Al−Al bond is not present. All the species were characterized on the basis of their IR spectra, taking into account the effects of isotopic substitution. The experiments were accompanied by quantum mechanical calculations relying on ab initio as well as DFT methods.

The experimental results are in good agreement with what is predicted by the calculations. The two molecules with the lowest relative energies according to our calculations, namely, the peroxo species $XAlO_2$ and the dioxo-bridged dimer $XAl(\mu\text{-}O)_2AlX$, were found to be the dominant products of the reactions in the experiments.

The experiments also give evidence for the formation of an additional species due to the reaction of AlX with more than one O_2 molecule. This species, which exhibits the formula $XAlO_4$, will be the topic of a separate paper.[27]

Acknowledgment. We thank the Deutsche Forschungsgemeinschaft for the award of a habilitation grant to H.-J.H. and for financial support.

IC011313D